**Pushing the boundaries of chemistry?
It takes
#HumanChemistry**

Make your curiosity and talent as a chemist matter to the world with a specialty chemicals leader. Together, we combine cutting-edge science with engineering expertise to create solutions that answer real-world problems. Find out how our approach to technology creates more opportunities for growth, and see what chemistry can do for you at:

evonik.com/career

EVONIK
Leading Beyond Chemistry

VIP *Very Important Publication*

Aromatic C–H Hydroxylation Reactions with Hydrogen Peroxide Catalyzed by Bulky Manganese Complexes

Eduard Masferrer-Rius,[a] Margarida Borrell,[b] Martin Lutz,[c] Miquel Costas,[b] and Robertus J. M. Klein Gebbink[a,*]

[a] Organic Chemistry and Catalysis, Debye Institute for Nanomaterials Science, Utrecht University, Universiteitsweg 99, 3584 CG Utrecht, The Netherlands
Phone: (+31)-30-2531889;
E-mail: r.j.m.kleingebbink@uu.nl
[b] Institut de Química Computacional i Catàlisi (IQCC) and Departament de Química, Universitat de Girona, Campus Montilivi, E-17071 Girona, Catalonia, Spain
[c] Structural Biochemistry, Bijvoet Centre for Biomolecular Research, Utrecht University, Padualaan 8, 3584 CH Utrecht, The Netherlands

Supporting information for this article is available on the WWW under https://doi.org/10.1002/adsc.202001590

Abstract: The oxidation of aromatic substrates to phenols with H_2O_2 as a benign oxidant remains an ongoing challenge in synthetic chemistry. Herein, we successfully achieved to catalyze aromatic C–H bond oxidations using a series of biologically inspired manganese catalysts in fluorinated alcohol solvents. While introduction of bulky substituents into the ligand structure of the catalyst favors aromatic C–H oxidations in alkylbenzenes, oxidation occurs at the benzylic position with ligands bearing electron-rich substituents. Therefore, the nature of the ligand is key in controlling the chemoselectivity of these Mn-catalyzed C–H oxidations. We show that introduction of bulky groups into the ligand prevents catalyst inhibition through phenolate-binding, consequently providing higher catalytic turnover numbers for phenol formation. Furthermore, employing halogenated carboxylic acids in the presence of bulky catalysts provides enhanced catalytic activities, which can be attributed to their low pK_a values that reduces catalyst inhibition by phenolate protonation as well as to their electron-withdrawing character that makes the manganese oxo species a more electrophilic oxidant. Moreover, to the best of our knowledge, the new system can accomplish the oxidation of alkylbenzenes with the highest yields so far reported for homogeneous arene hydroxylation catalysts. Overall our data provide a proof-of-concept of how $Mn(II)/H_2O_2/RCO_2H$ oxidation systems are easily tunable by means of the solvent, carboxylic acid additive, and steric demand of the ligand. The chemo- and site-selectivity patterns of the current system, a negligible KIE, the observation of an NIH-shift, and the effectiveness of using ^tBuOOH as oxidant overall suggest that hydroxylation of aromatic C–H bonds proceeds through a metal-based mechanism, with no significant involvement of hydroxyl radicals, and via an arene oxide intermediate.

Keywords: Aromatic C–H oxidation; Bioinspired oxidation; Fluorinated alcohol solvents; Halogenated carboxylic acids; Manganese catalysts; Phenols

Introduction

Oxidations of organic compounds are essential reactions widely studied in academia as well as in the chemical industry. The interest mainly arises from the fact that the oxygenated organic molecules can be further used to produce different classes of valuable chemicals, such as pharmaceuticals. Despite many

research efforts, the selective oxidation of organic substrates still represents a critical challenge in synthetic chemistry. For instance, the direct one-step hydroxylation of aromatic molecules to the corresponding phenols could provide easy access to relevant building blocks for more complex molecules, thereby representing a highly desired reaction.

To date, several bioinspired iron and manganese complexes have been shown to perform aliphatic C–H oxidations[1] as well as olefin oxidation reactions,[2] whereas hydroxylation of aromatic compounds has remained an ongoing issue since recent years.[3] In earlier studies, an iron complex supported by the tpa ligand (tpa = tris(2-pyridylmethyl)amine) was found to be capable of stoichiometrically oxidizing ligated perbenzoic acids through the self-hydroxylation of the aromatic ring, forming iron(III)-salicylate complexes.[3a] Also, an iron complex based on the bpmen ligand (bpmen = *N,N'*-dimethyl-*N,N'*-bis(2-picolyl)ethylenediamine) showed activity for the hydroxylation of aromatic compounds using H_2O_2, although strong coordination of phenolates to the iron(III) center prevented efficient catalysis.[3b,d] An iron complex supported by a N-heterocyclic carbene ligand has been shown to be cable of hydroxylating benzene and alkylbenzenes with H_2O_2 as well, albeit at low conversions and yields for phenol products, and with the formation of benzylic oxidized products from alkylbenzene substrates.[3e,h] Recent research progress indicates that iron complexes supported by bpbp-type ligands (bpbp = *N,N'*-bis(2-pyridylmethyl)-2,2'-bipyrrolidine) can hydroxylate aromatic substrates with H_2O_2.[3i,j,o] However, overoxidation products and modest selectivities for oxidation of the aromatic ring were observed, resulting in mixtures of products in which oxidation has taken place on aromatic as well as aliphatic positions. A manganese complex supported by the Bn-TPEN ligand (Bn-TPEN = *N*-benzyl-*N,N'N'*-tris(2-pyridylmethyl)-1,2-diaminoethane) has been found to oxidize naphthalene, among other substrates, with iodosylbenzene as oxidant.[3p] However, efficient catalytic turnover numbers (TON) were not achieved. Later, a manganese tpa complex incorporated into mesoporous silica-alumina was described to be active in the selective hydroxylation of benzene derivatives with H_2O_2.[3q] Interestingly, incorporation of the complex into the mesoporous support was necessary to get useful catalytic activities. Very recently, intramolecular aromatic hydroxylation, as well as intermolecular hydroxylation of benzene to phenol, has been demonstrated with an iron complex based on the Bn-TPEN ligand through O–O bond heterolysis of an Fe(III)–OOH species to form an Fe(V)=O oxidant.[3n]

Other transition-metal complexes have also been developed as homogeneous catalysts for aromatic C–H oxidations with H_2O_2 as the oxidant.[4] Itoh *et al.* demonstrated the catalytic ability of a nickel complex

supported by a tripodal tetradentate aminopyridine ligand in the direct hydroxylation of aromatics using a significant excess of oxidant (Figure 1).[4a] High TONs were only achieved using extremely low concentrations of catalyst under long reaction times; yet, absolute yields of phenol products did not exceed 7.5%. Remarkably though, when the complex was used at 10 mol% loading with respect to the substrate, 21% phenol yield was formed (2 turnovers per nickel).[4a,5] Later, Kodera *et al.* described a dinuclear copper complex as catalyst for the hydroxylation of aromatics, showing good selectivities for phenol products (Figure 1).[4b] Again, an elevated TON (12,550) was obtained at a low catalyst concentration, with phenol yields up to 21% for benzene oxidation. Di Stefano *et al.* reported an iminopyridine iron complex capable of oxidizing aromatic substrates, as well as aromatic amino acids, under mild reaction conditions (Figure 1).[3g,6] However, for all these examples, aromatic oxidation of alkylbenzenes is effectively accompanied by benzylic hydroxylation. In addition, recently reported nickel, copper and cobalt complexes supported by aminopyridine ligands accomplished the oxidation of benzene to phenol in improved yields (29–41%) (Figure 1).[4e–g]

Previously, we have shown that bulky iron complexes with tips moieties (tips = *tris*-(isopropyl)silyl) catalyze the site-selective oxidation of alkyl C–H bonds with H_2O_2, affording high product yields and enhanced preferential oxidation of secondary over tertiary C–H bonds.[1i] Likewise, manganese complexes supported by aminopyridine ligands catalyze chemo- and enantioselective aliphatic C–H oxidations with H_2O_2.[1f,j,k,o–r,t,7] Recently, White *et al.* reported that a
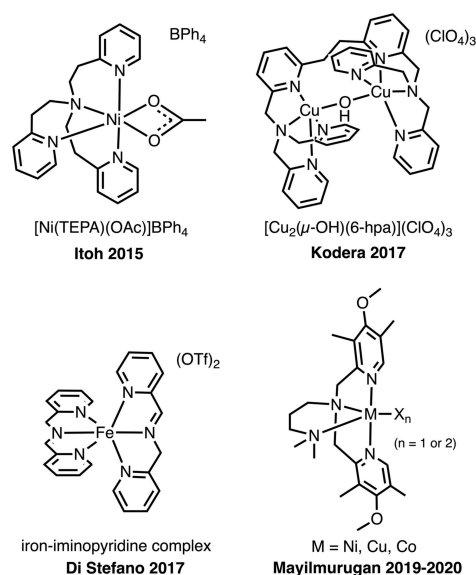

Figure 1. Examples of metal complexes previously employed in aromatic C–H hydroxylation reactions with H_2O_2.

bulky manganese complex with pendant *o*-CF$_3$-substituted aryl rings can oxidize methylene groups in the presence of aromatic functionalities.[1u] The authors also report non-productive aromatic substrate oxidation as a side-reaction. Finally, fluorinated alcohols have recently been shown to be suitable solvents for oxidation chemistry, preserving the first-formed alcohol products and, thus, reducing overoxidation reactions.[1o,7a,8]

Herein, we focus on the use of bioinspired manganese complexes for the oxidation of aromatic substrates. We demonstrate that the application of bulky Mn catalysts in the presence of fluorinated alcohol solvents favors oxidation at the aromatic ring over the oxidation of benzylic positions, providing an improved route to produce phenols. On the basis of previous literature examples which propose that product inhibition through metal-phenolate binding prevents catalytic turnover in aromatic oxidation reactions, we rationalized that the presence of bulky tips groups in position 5 of the pyridine rings may help in preventing product inhibition. Our study also shows that the yields of the aromatic reactions are further improved by using halogenated carboxylic acids as additives, which in part can be attributed to their lower pK$_a$ values which reduces product inhibition through a favorable acid-base equilibrium between the carboxylic acid and the (substituted) phenol products. Overall, our study has resulted in the development of a selective manganese-based catalyst system that performs arene hydroxylation reactions with H$_2$O$_2$ as a benign oxidant with improved yields of (substituted) phenol products with respect to the previously described homogeneous catalysts.

Results and Discussion

Aliphatic *vs* Aromatic C–H Oxidation

For our study we have investigated complexes of the type [M(OTf)$_2$(L)] based on the bpmcn, bpbp, bpbi and bpmen ligand families (Scheme 1) (bpmcn = *N,N'*-dimethyl-*N,N'*-bis(2-picolyl)-cyclohexane-*trans*-1,2-diamine, bpbi = *N,N'*-bis(2-picolyl)-2,2'-bis-isoindoline). We have included manganese complexes containing electron-rich, as well as bulky pyridines.
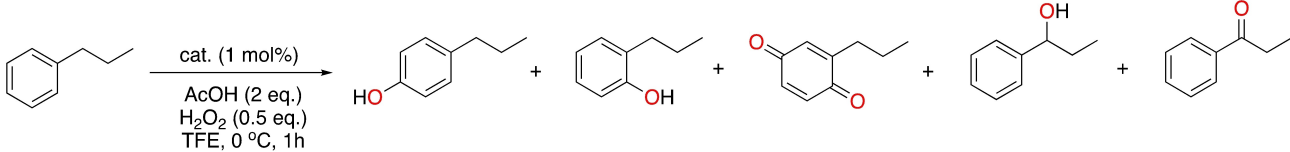
Initially, we focused our attention on the hydroxylation of propylbenzene as substrate using 1 mol% of **Mn(^{tips}bpmcn)**, **Mn(^{dMM}bpmcn)**, or **Mn(bpmcn)** as catalyst (Table 1). Catalytic oxidation reactions were carried out by mixing the Mn(II) catalyst and AcOH (2 equiv.) into a solution of propylbenzene (1 equiv.) in TFE (TFE = 2,2,2-trifluoroethanol) at 0 °C. A substoichiometric amount of aqueous H$_2$O$_2$ (0.5 equiv., 35% w/w solution) was added dropwise through a syringe pump over a period of 30 min. Interestingly, chemoselectivity was found to be largely dependent on the catalyst used. The bulky manganese complex **Mn(^{tips}bpmcn)** favors the oxidation at the aromatic ring, providing the *para*-phenol as the major product, together with *ortho*-phenol and propyl-*p*-benzoquinone as minor products. Some 1-phenyl-1-propanol was also detected as minor product in this case, showing a ratio of aromatic:aliphatic oxidation of 7.3:1. In contrast, when the electron-rich catalyst **Mn(^{dMM}bpmcn)** was used the chemoselectivity changed completely, and preference for the oxidation at the benzylic position was observed with a ratio of aromatic:aliphatic oxidation products of 1:13.5. This observation is in agreement with previous reports on the use of electron-
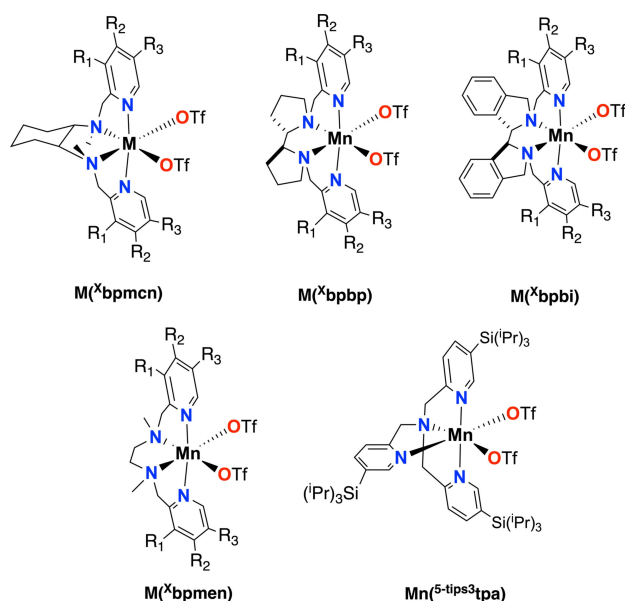
	R$_1$	R$_2$	R$_3$
Mn(bpmcn)	-H	-H	-H
Mn(^{dMM}bpmcn)	-Me	-OMe	-Me
Mn(^{tips}bpmcn)	-H	-H	-Si(^{i}Pr)$_3$
Fe(^{tips}bpmcn)	-H	-H	-Si(^{i}Pr)$_3$
Mn(bpbp)	-H	-H	-H
Mn(^{dMM}bpbp)	-Me	-OMe	-Me
Mn(^{tips}bpbp)	-H	-H	-Si(^{i}Pr)$_3$
Mn(bpbi)	-H	-H	-H
Mn(^{tips}bpbi)	-H	-H	-Si(^{i}Pr)$_3$
Mn(bpmen)	-H	-H	-H
Mn(^{tips}bpmen)	-H	-H	-Si(^{i}Pr)$_3$

Scheme 1. Manganese and iron complexes employed in this work.

Table 1. Oxidation of propylbenzene in TFE with different manganese catalysts.

Catalyst	r.s.m[a]	p-Phenol[b]	o-Phenol[b]	Quinone[b]	Alcohol[b]	Ketone[b]	MB[c]	Ratio[d]
Mn(^{tips}bpmcn)	68	9 (18)	1 (3)	2 (8)	2 (4)	n.d.	88	7.3:1
Mn(^{dMM}bpmcn)	65	1 (2)	n.d.	n.d.	12 (23)	1 (4)	85	1:13.5
Mn(bpmcn)	72	3 (6)	1 (2)	3 (11)	4 (9)	n.d.	89	2.1:1

[a] Remaining starting material (r.s.m) in %.

[b] Yields in % with respect to substrate determined by GC against an internal standard. In parenthesis yields in % with respect to H_2O_2. Yields are calculated considering that 2 equiv. of H_2O_2 are necessary for the formation of the ketone and quinone products.

[c] Mass balance (MB) was calculated considering remaining starting material and all products formed, plus a percentage of substrate loss calculated with blank experiments (an average of 6% of substrate is lost): MB = (r.s.m %) + (Product Yields %) + (Substrate loss).

[d] Ratio (aromatic:aliphatic) = [n(p-phenol) + n(o-phenol) + n(quinone)]/[n(alcohol) + n(ketone)]. n.d. = non-detected.

rich manganese complexes for asymmetric benzylic oxidations, where no aromatic oxidation products were detected.[1o,7a,8f] With the parent **Mn(bpmcn)** complex, we observed both oxidation at the aromatic ring as well as at the benzylic position in a ratio of 2.1:1, respectively, showing a slight preference for aromatic oxidation.

Worthy of note are the blue colors that progressively form in the reaction mixtures after starting the addition of H_2O_2 to the reaction mixture containing the substrate and the catalyst (**Mn(^{tips}bpmcn)** or **Mn-(bpmcn)**). We hypothesize that these colors are due to charge transfer bands arising from phenolate binding to the Mn center, which in turn inhibits the catalyst and prevents further catalytic turnover.[9] Consistent with this hypothesis, ESI-MS analysis of a mixture of **Mn(^{tips}bpmcn)** (1 mol%), *tert*-butylbenzene (1 equiv.), AcOH (2 equiv.) and H_2O_2 (1 equiv.) at 0 °C in TFE showed a main peak at *m/z* = 493.8060, which corresponds to the formation of a complex ion composed of a **Mn(^{tips}bpmcn)** fragment and a coupled bis(phenolate) fragment ([Mn(^{tips}bpmcn)(C$_6$H$_3$OC-(CH$_3$)$_3$)$_2$]$^{2+}$, calcd *m/z* 493.8064) (SI, Section 5.7, Figure S11). Importantly, the blue color was observed immediately after the start of H_2O_2 addition in the case of **Mn(bpmcn)**, whereas for the reaction with **Mn-(^{tips}bpmcn)** the blue color appears later in the course of the reaction. These observations lead us to believe that the bulky tips groups help in preventing phenolate binding, and thus allow for higher catalytic turnover numbers. A control experiment without an aromatic substrate did not show the appearance of the blue colors described above.

Comparing our result on arene hydroxylation catalyzed by **Mn(^{tips}bpmcn)** with previous literature examples, such as the systems described by Itoh[4a] and

Kodera,[4b] we can conclude that the current system performs the hydroxylation of an alkylbenzene with yields commensurate to state-of-the-art homogeneous catalysts, at a relatively low catalyst loading. Furthermore, the nature of the ligand in the current system seems key for diverting the chemoselectivity of the catalyst from oxidation of the more activated benzylic position to the hydroxylation of the aromatic ring, showing a catalyst dependent selectivity. Yet, overall the reactions shown in Table 1 suffer from moderate conversions and yields, but do show reasonable mass balances. Noteworthy is that blank experiments without catalyst showed that a certain amount of substrate is lost during the reaction and analysis protocol (~6%). This loss was taken into account to calculate the mass balances in Table 1.
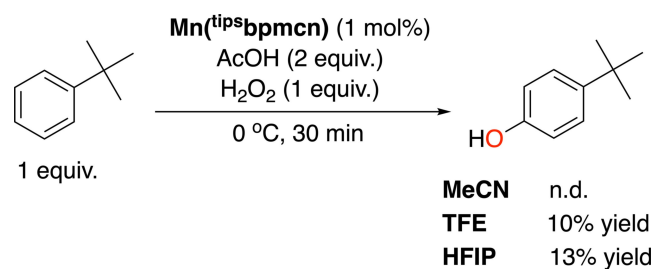
Screening of Catalysts

Based on these results, we selected bulky manganese complexes with different amine backbones for further screening for the oxidation of aromatic C–H bonds (Scheme 1). A bulky iron complex, **Fe(^{tips}bpmcn)**, was also included in our study. The parent complexes without any substituents on the pyridines were considered as well. For all cases, the metal center adopts a C$_2$-symmetric *cis*-α topology, with the two pyridines *trans* to each other. A new manganese complex supported by a bulky tripodal tetradentate ligand based on the tpa motif ($^{5-tips3}$tpa)[2m] was also included.

Tert-butylbenzene was used as a model substrate since it lacks benzylic C–H bonds to selectively screen for activity in aromatic oxidation. Using stoichiometric amounts of H_2O_2, crude mixtures were analyzed by GC, detecting mainly 4-*tert*-butylphenol as the oxidized product, next to unreacted substrate. Interest-

ingly, no *ortho*-hydroxylation product was observed, which is in contrast to, *e.g.*, the oxidation of *tert*-butylbenzene catalyzed by an iminopyridine Fe(II) complex.[3g] In general, poor mass balances were observed for these reactions. We believe that a side reaction might happen, leading to overoxidized by-products, which we have not been able to identify yet. However, interest was focused here on the formation of the phenol product. First, a screening of different solvents was done (Scheme 2). Next to TFE, HFIP (HFIP = 1,1,1,3,3,3-hexafluoro-2-propanol) was found to be an appropriate solvent as well, allowing similar phenol formation as TFE. Interestingly, acetonitrile is not a suitable solvent, showing no formation of the desired phenol product. The positive effect of using fluorinated alcohol solvents may be attributed to their strong hydrogen donor ability, which decreases the nucleophilicity of the phenol, thereby allowing higher catalytic turnover numbers by hampering product inhibition. These findings inspired us to use manganese complexes in the presence of fluorinated alcohol solvents in further investigations.

Next, we proceeded to screen the different complexes shown in Scheme 1 using TFE as the solvent (SI, Table S1). Overall, complexes bearing bulky, tips-appended ligands exhibited a better catalytic activity, showing higher conversion and phenol production compared to their parent complexes. Maximum yields for the 4-*tert*-butyphenol product were obtained using **Mn(tipsbpmcn)**, **Mn(tipsbpbi)**, and **Mn(tipsbpmen)** (SI, Table S1, entry 2, 7 and 9), whereas the other complexes show good conversions but lower yields. The current findings suggest the relevance of steric effects in aromatic hydroxylation reactions, whereas electronic effects may play a less important role. We believe that product inhibition in complexes with bulky ligands occurs to a lower extent in comparison to complexes with non-bulky ligands. Besides, iron complex **Fe-(tipsbpmcn)**, supported by a bulky bpmcn ligand, provided a poor yield (SI, Table S1, entry 3). Iron complexes with N4 ligands have been reported as catalysts for aromatic oxidation by Bryliakov and co-workers.[3j,k] Yet, we believe that product inhibition in these catalysts through phenolate-iron coordination is more prominent than with our manganese complexes,

which translates in a much lower catalytic efficiency for the iron catalysts. Accordingly, we focused our study exclusively on the use of manganese complexes as catalysts. Complex **Mn(5−tips3tpa)**, which bears a sterically encumbered tripodal tetradentate aminopyridine ligand based on the tpa scaffold, also provided a poor 4-*tert*-butylphenol yield (SI, Table S1, entry 11), indicating that the use of linear tetradentate aminopyridine ligands with a *cis-α* topology seems preferred over the use of tripodal ligands. Manganese triflate was also tested as catalyst, showing no reaction.

Catalyst **Mn(tipsbpmcn)** was then chosen for further reaction optimization (SI, Table S2) since it showed the better selectivity for phenol production. However, at this point yields for phenol product were still modest (up to 15% yield).

Carboxylic Acid Additives

Carboxylic acids have been investigated in detail as additives in H_2O_2-mediated oxidation catalysis. We found that very low phenol product formation was observed when the oxidation of *tert*-butylbenzene was run without the addition of any carboxylic acid, showing that this additive is crucial for reactivity (Table 2, entry 1). As previously discussed in the literature, catalysis might proceed through a "carboxylic acid-assisted" pathway, in which the acid helps in the heterolytic cleavage of the O—O bond of a Mn(III) hydroperoxo intermediate to form a Mn(V) oxo

Table 2. Oxidation of *tert*-butylbenzene using different carboxylic acids.[a]

Entry	Carboxylic acid (2 equiv.)	4-*tert*-butylphenol yield (%)[b]
1	–	4
2	Acetic acid	13
3	Propionic acid	6
4	Butyric acid	6
5	Isobutyric acid	3
6	Pivalic acid	1
7	2-ethylhexanoic acid	5
8	Chloroacetic acid	26
9	Dichloroacetic acid	29
10	Trichloroacetic acid	2
11	Fluoroacetic acid	26
12	Difluoroacetic acid	21
13	Trifluoroacetic acid	n.d.
14	Iodoacetic acid	6
15	*N,N*-dimethylglycine	2
16	2-nitrobenzoic acid	23
17	3-nitrobenzoic acid	25

[a] Reaction conditions: **Mn(tipsbpmcn)**:H_2O_2:substrate: RCO_2H = 1:100:100:200, in HFIP at 0 °C.
[b] Conversion and yields determined from crude reaction mixtures by GC. n.d. = non-detected.

Scheme 2. Oxidation of *tert*-butylbenzene in different solvents.

Reaction shown: *tert*-butylbenzene (1 equiv.) → 4-*tert*-butylphenol, with
Mn(tipsbpmcn) (1 mol%)
AcOH (2 equiv.)
H_2O_2 (1 equiv.)
0 °C, 30 min

MeCN	n.d.
TFE	10% yield
HFIP	13% yield

species, responsible for the oxidation of the aromatic substrate.[1m,10] Alternatively, the acid could also help in C–H bond activation, as in acetate-assisted C–H activation with palladium.[11] Since the introduction of bulky substituents in the ligand has been found to be a key feature in order to obtain catalytic turnover, several bulkier carboxylic acids were tested. Carboxylic acids with longer alkyl chains, *i.e.* propionic acid and butyric acid, showed lower phenol formation compared to acetic acid (Table 2, entries 3 and 4). When bulkier carboxylic acids such as isobutyric acid, pivalic acid, and 2-ethylhexanoic acid were tested, yields for the desired oxidized product also decreased (Table 2, entries 5, 6 and 7). Therefore, our findings show that the introduction of bulk into the carboxylic acid additive decreases product formation. Similar trends were observed when either HFIP or TFE were used as solvent (SI, Table S3-S6 and Figure S3-S6).

Next, we considered the use of halogenated carboxylic acids, which have been used previously in oxidation reactions.[1u,7d,12] Interestingly, we have found that chloroacetic acid, dichloroacetic acid, fluoroacetic acid, and difluoroacetic acid afford a significant increase in yield for the desired phenol product, with up to 29% 4-*tert*-butylphenol yield (Table 2, entry 9). The reason of this improvement could be related to the pK_a of the carboxylic acids, which varies significantly within the series of tested aliphatic carboxylic acids. The role of the lower pK_a of these carboxylic acids in arene hydroxylation reactions could be twofold. First, it keeps the phenol products protonated, which hampers catalyst deactivation by phenolate binding. Second, the electron-withdrawing character of these acids makes the proposed Mn(V) oxo species more electrophilic, which may result in a more reactive oxidant towards arenes. The use of nitrobenzoic acids also lead to increased phenol formation compared to the use of acetic acid. However, in these cases side-product formation through arene hydroxylation of the nitrobenzoic acid was observed. In the presence of halogenated carboxylic acids higher catalytic activities were achieved in HFIP compared to TFE (SI, Table S3 and S6).

Increasing the acidity has a positive effect, going from acetic acid ($pK_a = 4.76$) to 3-nitrobenzoic acid ($pK_a = 3.46$), chloroacetic acid ($pK_a = 2.87$), fluoroacetic acid ($pK_a = 2.59$), 2-nitrobenzoic acid ($pK_a = 2.17$) and dichloroacetic acid ($pK_a = 1.35$) (Figure 2).[13] However, the use of trichloroacetic acid ($pK_a = 0.66$) or trifluoroacetic acid ($pK_a = 0.52$) lead to a dramatic decrease in catalytic activity, which might be due to protonation of the amine moieties of the ligand. Iodoacetic acid ($pK_a = 3.18$) provided good conversion but a poor phenol yield, which could be explained by the weaker C-halogen bond that may lead to side reactions (Table 2, entry 14). N,N-dimethylglycine was also not a suitable additive, showing
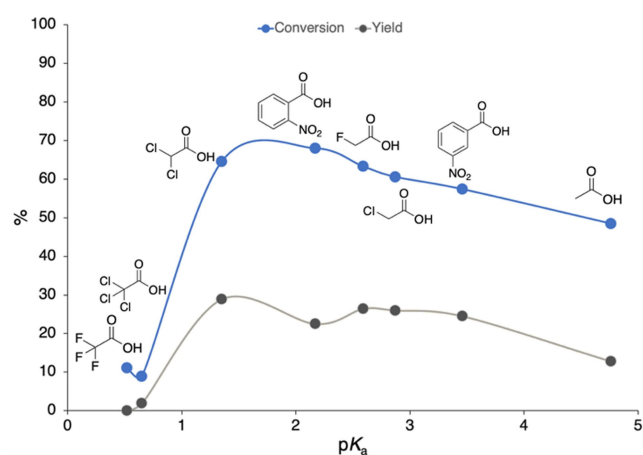

Figure 2. Effect of pK_a of the carboxylic acid additive on the hydroxylation of *tert*-butylbenzene. Reaction conditions: **Mn-(^{tips}bpmcn)**:H$_2$O$_2$:substrate:RCO$_2$H = 1:100:100:200, in HFIP at 0 °C.

poor yield for the desired phenol product, as well as low substrate conversion (Table 2, entry 15). Thus, we can conclude that steric bulk on the carboxylic acid additive is detrimental for the arene hydroxylation reaction, and that there is an optimum pK_a of the acid additive.

While it may be initially regarded as a modest value, the 29% yield obtained for 4-*tert*-butylphenol in a completely site selective manner is remarkable when compared with literature precedents; a recently reported iminopyridine Fe(II) catalyst has been shown to be capable of oxidizing *tert*-butylbenzene to 4-*tert*-butylphenol in 23% yield, together with the *ortho*-phenol and benzoquinone as minor products, which at that time were the highest numbers reported for *tert*-butylbenzene oxidation.[3g]

Further investigations on the effect of halogenated carboxylic acids showed that the conversion and yield do not drastically change between 0.5 to 8 equiv. of acid when **Mn(^{tips}bpmcn)** is used as catalyst (SI, Table S5 and Figure S5). This allows catalysis to be performed at a much lower carboxylic acid loading.

Next, bulky manganese complexes with different amine backbones in the ligand structure were tested in the aromatic hydroxylation of *tert*-butylbenzene using optimized chloro- and dichloroacetic acid loadings (Figure 3). The use of chloroacetic acid afforded similar efficiencies for the four catalysts tested, **Mn-(^{tips}bpmcn)** being the one that showed better conversion and yield. For dichloroacetic acid, we observed that **Mn(^{tips}bpmcn)** and **Mn(^{tips}bpbp)** performed best, with **Mn(^{tips}bpmcn)** showing significantly higher conversion and yield. In contrast, **Mn(^{tips}bpbi)** and **Mn-(^{tips}bpmen)** showed very poor results when using dichloroacetic acid. A similar reactivity trend was observed when TFE was used as solvent (SI, Table S7
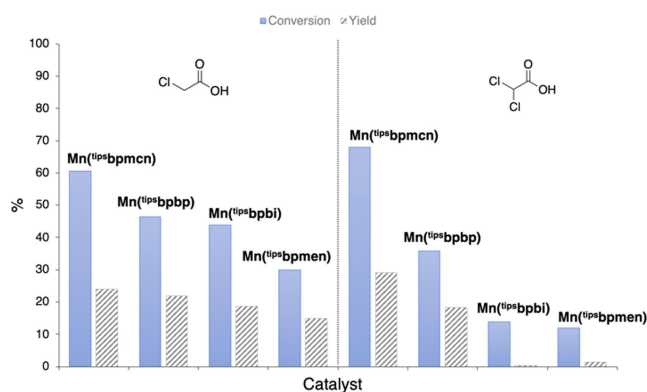
Figure 3. Effect of different amine ligand backbones on the Mn-catalyzed hydroxylation of *tert*-butylbenzene. Reaction conditions: Mn-cat.:H_2O_2:substrate:$RCO_2H = 1:100:100:50$, in HFIP at 0 °C (blue bars represent substrate conversion and grey bars 4-*tert*-butylphenol yield).

and Figure S9). Therefore, we can conclude that the amine backbone in the ligand structure of the manganese complexes has a considerable impact on catalytic activity. Besides, we believe that the simpler ethylene diamine backbone is less stable under acidic conditions, since with dichloroacetic acid as additive a poor 4-*tert*-butylphenol yield is afforded. Consistent with this hypothesis, this complex is more efficient under low carboxylic acid loadings; hydroxylation of *tert*-butylbenzene with **Mn(ᵗⁱᵖˢbpmen)** leads to only 6% 4-*tert*-butylphenol yield when 2 equivalents of chloroacetic acid are used, whereas 15% yield is obtained with 0.5 equiv. of the acid.

Finally, we have further investigated the role of the halogenated carboxylic acid additives by examining the use of dichloroacetic acid with different manganese complexes for the hydroxylation of propylbenzene, this time at a low H_2O_2 loading (SI, Table S11). Our earlier findings showed that for **Mn(ᵗⁱᵖˢbpmcn)** the use of dichloroacetic acid provides an enhanced catalytic activity compared to the use of AcOH (compare Tables 1 and S11). On the other hand, for the electron-rich complex **Mn(ᵈᴹᴹbpmcn)** a complete change in chemoselectivity from aliphatic to aromatic hydroxylation was observed when switching to dichloroacetic acid, albeit at low yields (compare Tables 1 and S11). For the parent complex **Mn(bpmcn)** an increased activity for aromatic hydroxylation was observed when dichloroacetic acid was employed instead of AcOH. Remarkably, traces of 1-phenyl-1-propanol were detected for all these catalysts when dichloroacetic acid was employed, revealing that the use of a halogenated carboxylic acid increases the selectivity towards the oxidation of aromatic C–H bonds for these complexes in a general sense, avoiding the generation of products originating from oxidation at a more activated benzylic position.
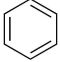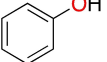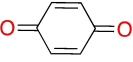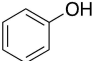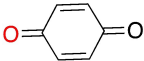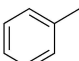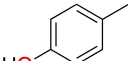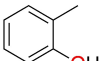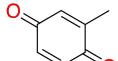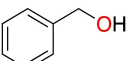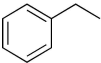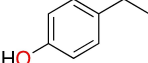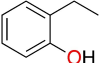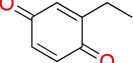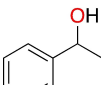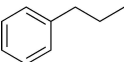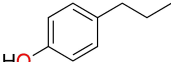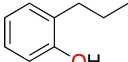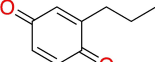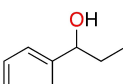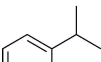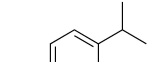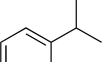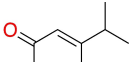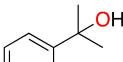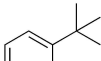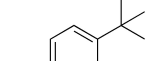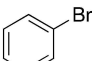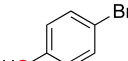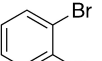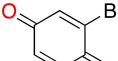
Substrate Scope

Aromatic C–H hydroxylation of different substrates has been explored under the optimized experimental conditions using the manganese complex **Mn-(ᵗⁱᵖˢbpmcn)** (Table 3). For comparison purposes, some of the best results described so far in the literature with transition-metal complexes are collected in Tables S9 and S10. In general, our current Mn(II)/H_2O_2/$Cl_2CHCOOH$ catalytic system affords higher yields and substantially improved selectivities for aromatic over aliphatic C–H oxidation.

At first, we considered benzene as substrate, which leads to phenol in a remarkable yield of 32%, along with *para*-benzoquinone in 7% yield (Table 3, entry 1). Interestingly, when phenol was used as the substrate, 13% yield of *para*-benzoquinone was observed, showing that the primary oxidation product in benzene hydroxylation can indeed engage in a second oxidation step (Table 3, entry 2). Next, we extended our study to the oxidation of alkylbenzenes. Oxidized products were obtained in remarkable total product yields ranging from 29 to 37%, with the *para*-phenol as the main product in all cases, which is reminiscent to reactions proceeding via an electrophilic aromatic substitution type of mechanism. Toluene was oxidized to *para*-cresol in 22% yield, together with *ortho*-cresol and methyl-*para*-benzoquinone in 8 and 1% yield, respectively (Table 3, entry 3). Recent studies on aromatic oxidations have shown other complexes to be capable of oxidizing the aromatic ring of toluene as well, showing however significant amounts of aliphatic oxidation towards benzyl alcohol or benzaldehyde products.[3g,4a,b,e,f] Remarkably, **Mn(ᵗⁱᵖˢbpmcn)** shows an excellent selectivity for oxidation of the aromatic ring over the aliphatic site chain. Oxidation of other alkylbenzene derivatives with more reactive benzylic C–H bonds was also explored. Ethylbenzene provided 4-ethylphenol as the major product in 26% yield, along with 2-ethylphe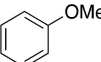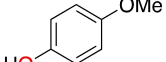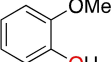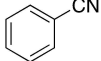nol and ethyl-*para*-benzoquinone in 8 and 2% yield, respectively (Table 3, entry 4). For the oxidation of propylbenzene, we observed 4-propylphenol, 2-propylphenol and propyl-*para*-benzoquinone in 24, 8, and 2% yield, respectively (Table 3, entry 5).

Cumene was also considered, which bears a more encumbered isopropyl substituent with a weak 3⁰ benzylic C–H bond. 4-Isopropylphenol and 2-isopropylphenol were obtained in 30 and 5% yield, respectively. Minor amounts of isopropyl-*para*-benzoquinone were detected in 2% yield (Table 3, entry 6). To the best of our knowledge, hydroxylation of this group of alkylbenzene substrates catalyzed by the current system provides the highest yields reported to date with homogeneous catalysts. Remarkably, only traces of benzylic oxidation products were detected in these reactions, suggesting that the current catalytic system is selective for aromatic hydroxylation reac-

Table 3. Product analysis in the oxidation of benzene and its derivatives catalyzed by **Mn(tipsbpmcn)**[a]

Entry	Substrate (r.s.m %)[b]	p-Phenol (%)[c]	o-Phenol (%)[c]	Quinone (%)[c]	Benzylic oxidation (%)[d]	Mass balance (%)[e]
1	44	32	–	7	–	88
2	70	–	–	13	–	86
3	49	22	8	1	traces	80
4	34	26	8	2	traces	71
5	45	24	8	2	traces	81
6	38	30	5	2	traces	75
7	32	29	–	–	–	66
8	45	8	14	5	–	72
9	84	6	4	–	–	94[f]
10	> 99	–	–	–	–	> 99[f]

[a] Reaction conditions: **Mn(tipsbpmcn)**:H_2O_2:substrate:$Cl_2CHCOOH$ = 1:100:100:50, in HFIP at 0 °C for 30 min.
[b] Remaining starting material (r.s.m.) determined from crude reaction mixtures by GC.
[c] Product yields determined from crude reaction mixtures by GC.
[d] Benzaldehyde or ketone products were not detected.
[e] Mass balance was calculated considering remaining starting material and all products formed, plus a percentage of substrate loss calculated from blank experiments: MB = (r.s.m %) + (Product Yields %) + (Substrate loss %).
[f] Percentage of substrate loss was not calculated.

tions. A cautious note must be introduced at this point because some of these compounds show the lowest mass balance of all substrates tested in this study, which raises the possibility that benzylic oxidation products are also formed but overoxidized to non-detected products. Important to note is that no formation of ketone products was observed, *i.e.* secondary oxidation of initial benzylic alcohol products does not seem to take place. Blank experiments without catalyst were done to calculate the amount of substrate loss during the reactions, and were used to calculate the mass balances in Table 3.

We observed a correlation between the bulk of the lateral alkyl chain in the aromatic substrate and the product profile. Our results clearly show that increasing the bulk of the substituents on the substrate translates into a decreased formation of *ortho*-phenol product, which is likely due to steric effects of both the catalyst and the substrate. The amounts of *ortho*-phenol were similar for toluene, ethylbenzene, and propylbenzene. However, when a bulkier substrate, such as cumene, was used, the yield for the *ortho*-phenol decreased. More remarkable is the oxidation of *tert*-butylbenzene, where no *ortho*-phenol product was detected at all, *i.e.* 4-*tert*-butylphenol was detected as the only product in 29% yield (Table 3, entry 7). The current data contrast with the oxidation of cumene catalyzed by a Ni(II) complex supported by an aminopyridine ligand, where mixtures of *ortho*-, *meta*- and *para*-phenols were obtained together with benzylic oxidized products, albeit in very low yields.[4a] Thus, our data indicate the importance of steric catalyst effects to dictate the regioselectivity of the hydroxylation reaction.

Using bromobenzene as substrate, 2-bromophenol and 4-bromophenol were obtained in 14 and 8% yield, respectively. 2-Bromo-1,4-benzoquinone was also detected in 5% yield (Table 3, entry 8). The formation of *ortho* and *para* phenols is in agreement with classical aromatic substitution reactions, halogen and alkyl substituents being *ortho* and *para* directing groups. However, of importance is the different selectivity observed for bromobenzene compared to the alkylbenzene substrates; where the *ortho*-phenol was obtained as the main oxidized product in the former case, the *para*-phenol was the major product in the latter case.

An electron-donating substituent was expected to enhance the reactivity of the arene substrate in our system. Nonetheless, anisole showed a poor reactivity, with 4-methoxyphenol and 2-methoxyphenol being produced in only 6 and 4% yield, respectively (Table 3, entry 9). No benzoquinone was detected in this case. For benzonitrile, bearing an electron-withdrawing cyano group, no oxidized products were detected (Table 3, entry 10). While the cyano group could deactivate the aromatic ring towards electrophiles, the coordinating ability of the methoxy and cyano groups
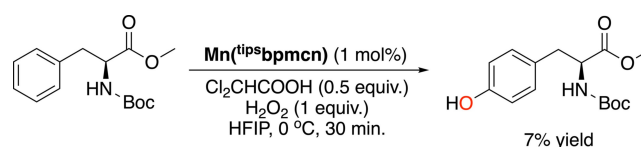

Scheme 3. Aromatic C–H hydroxylation of a natural product.

in anisole and benzonitrile might also interfere with catalysis. We believe that the poor catalytic activity for anisole may be due to strong binding of the first formed hydroxylated product to the metal center (indicated by a strong color change to purple). Indeed, competitive experiments using equimolar amounts of anisole and *tert*-butylbenzene show only 2% 4-*tert*-butylphenol yield, demonstrating catalyst deactivation in the presence of anisole.

Amino acid substrates are particularly interesting because of their biological significance and their molecular complexity, containing different types of C–H bonds. We therefore examined the catalytic hydroxylation of phenylalanine. Our idea was to extrapolate the reactivity that we have observed using simple aromatic substrates to the oxidation of more complex molecules. Interestingly, we found that oxidation at the *para*-position of the aromatic ring of a protected phenylalanine yields the corresponding tyrosine as the main product in 7% yield, which represents 7 catalytic turn-overs per Mn (Scheme 3). The hydroxylation of phenylalanine might be further optimized by variation of reaction conditions and protecting groups.

Mechanistic Considerations

Finally, our efforts have been devoted to the understanding of the mechanism of the aromatic hydroxylation reaction. Generally, activation of H_2O_2 by manganese or iron complexes supported by aminopyridine ligands leads to electrophilic oxidants.[1h,2e,g,10a,b] It is proposed that the starting Mn(II) complex is first oxidized to a Mn(III) hydroperoxo species, which then converts to a Mn(V) oxo complex through O–O bond heterolysis,[1m,10a,b] this last step being assisted by the carboxylic acid additive (Scheme 4). We propose that the aromatic hydroxylation reaction occurs via a similar oxidizing species, without the involvement of oxygen-centered radicals. It is well-known that free radicals, such as hydroxyl radicals generated via a Fenton process, can perform the oxidation of aromatic C–H bonds, but show low efficiencies and selectivities.[14] The involvement of such radicals would lead to side products through lateral site chain oxidation in alkylbenzene derivatives, because these oxygen-centered radicals poorly discriminate between C–H bonds of different strengths.[3g,15] In addition, hydroxylation of alkylbenzenes via hydroxyl radicals
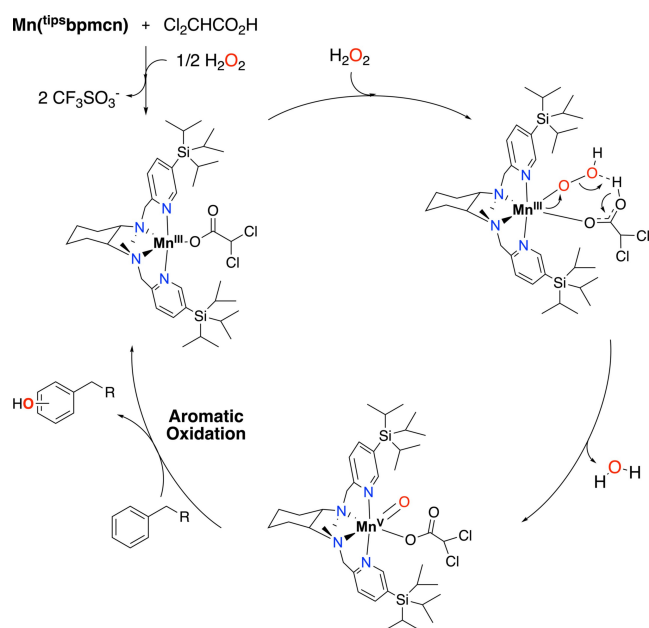
Scheme 4. Proposed mechanistic cycle based on the carboxylic acid assisted O–O cleavage of non-heme Fe and Mn complexes.[1h,m,2e,16]

give a specific distribution of *ortho*-, *meta*- and *para*-phenol isomers.[17] Several of our observations speak against the involvement of hydroxyl radicals in our aromatic hydroxylation reaction, and point towards a metal-based oxidation mechanism.

Our catalysis experiments show that oxidation of electron-rich benzene derivatives leads to the formation of *para* and *ortho* phenol products, with no formation of the *meta* isomer. This clearly contrasts with other catalysts capable of performing arene hydroxylation, such as the systems reported by Itoh,[4a] Bryliakov[3j] and Di Stefano,[3g] where mixtures of *ortho*-, *meta*- and *para*-phenols were observed (SI, Table S10); and thus, suggests that the current reaction undergoes through a more selective species. In contrast, when switching to electron-poor substrates, no aromatic hydroxylation reaction takes place with the current system. These observations agree with the proposal of an electrophilic manganese-oxo species, with a reactivity sensitive to the electronic nature of the substrate.

Previous studies have shown that the oxidation of toluene with hydroxyl radicals afford cresols with a distribution of 71:9:20 for *ortho*:*meta*:*para* isomers.[17] The current work has shown that the bulky **Mn-(**tips**bpmcn)** catalyst is capable of oxidizing toluene with high selectivity, affording a ratio of 27:0:73 for the *ortho*-, *meta*- and *para*-cresols, respectively. Therefore, our data clearly show a distinct distribution of isomers compared with the reaction involving hydroxyl

radicals, and consequently point towards the involvement of a metal-based mechanism.

To get further insight in the mechanism, we considered performing the hydroxylation reaction with another oxidant than H_2O_2. Remarkably, we found that catalytic hydroxylation of *tert*-butylbenzene by **Mn-(**tips**bpmcn)** in fluorinated alcohol solvents can also be accomplished employing ^{t}BuOOH as oxidant, generating 4-*tert*-butylphenol as the oxidized product in 9% yield. It is known that oxidations with ^{t}BuOOH can proceed through a Fenton-type process, generating free-diffusing *tert*-butoxy and *tert*-butylperoxy radicals that can engage in hydrogen abstraction reactions with aliphatic C–H bonds.[2e,18] However, ^{t}BuOOH activation does not produce hydroxyl radicals, and *tert*-butoxy radicals, unlike hydroxyl radicals, do not add to aromatic rings.[19] Another evidence against the involvement of hydroxyl radicals is that the aromatic hydroxylation reactions catalyzed by **Mn(**tips**bpmcn)** are not affected by the presence, or absence, of air. Independent experiments carried out under air and under a nitrogen atmosphere showed similar efficiencies for the generation of 4-*tert*-butylphenol (SI, Table S12). In contrast, a significant impact of air on product yields is observed when oxidations are mediated by oxygen-centered radicals.[3g,14c,d,20]

Next, we carried out a kinetic isotope effect (KIE) experiment using a 1:1 mixture of benzene and perdeuterated benzene as substrate and **Mn(**tips**bpmcn)** as catalyst. From the ratio of phenol to phenol-d_5, a KIE value of 0.97 ± 0.06 was determined for this reaction. This value rules out Fenton-type processes, for which a KIE of 1.7 has been reported.[21] Overall, our combined data suggest that aromatic hydroxylation reactions catalyzed by **Mn(**tips**bpmcn)** occur through a metal-based mechanism with no significant involvement of hydroxyl radicals. Besides, the high bond dissociation energy of aromatic C–H's discards a HAT initiated process. Instead, the data is consistent with an aromatic hydroxylation mechanism via electrophilic attack of the high valent metal oxo on the aromatic ring. As a first option, the KIE value found in this study is compatible with the formation of a Wheland type of intermediate found in an electrophilic aromatic substitution mechanism. Alternatively, an initial arene epoxidation reaction conducted by the high valent manganese-oxo species, followed by an acid catalyzed re-aromatization to form the corresponding phenol could be a plausible mechanism.[22] Both proposed processes show a negligible KIE, which is consistent with a change in hybridization from sp^2 to sp^3 of the aromatic carbon where the oxidation takes place.[3g,23]

To get further insight into the arene hydroxylation mechanism, we performed a catalytic experiment using 1-*tert*-butyl-4-deuterobenzene to probe the occurrence of an NIH shift (Scheme 5). This characteristic feature of arene hydroxylation reactions based on the migra-
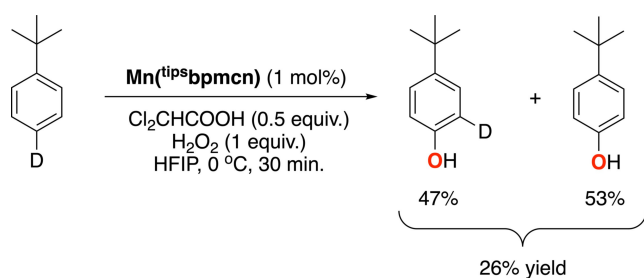
Scheme 5. Deuterium labeling study.

tion of a substituent from the formal hydroxylation site to an adjacent carbon position can indicate the involvement of an arene oxide as a reaction intermediate.[24] Based on our previous experiments, we know that hydroxylation of *tert*-butylbenzene only occurs at the *para*-position of the benzene ring. Combined GC and GC-MS analysis of the reaction with 1-*tert*-butyl-4-deuterobenzene indeed showed the exclusive formation of *para*-phenol products (26%), with a 4-*tert*-butyl-2-deuterophenol and 4-*tert*-butylphenol ratio of 47/53, indicating that an NIH-shift takes place during the reaction. On basis of this observation, we suggest that the aromatic hydroxylation reaction most likely occurs through an arene epoxidation mechanism, involving the generation of a cyclohexadienone intermediate after arene oxide formation.

We propose that the use of an electron-deficient acid can make the metal oxo species more electrophilic, which also reduces catalyst inhibition by phenolate protonation. These effects, together with a sterically demanding aminopyridine ligand, translate into an oxidizing agent which is reactive towards the *para*-position of the aromatic ring instead of the (benzylic) aliphatic C–H bonds. Overall, we believe that there is a synergy between the carboxylic acid and the manganese complex, as was recently also shown for methylene and tertiary C–H oxidation catalyzed by other manganese complexes with chloroacetic acid as additive.[1u,7d,25] Further investigations into the exact role of halogenated carboxylic acids are required to understand how chemoselectivity is governed in these aromatic hydroxylation reactions.

Conclusion

We have presented a new catalytic procedure for the direct one-step hydroxylation of aromatic C–H bonds to the corresponding phenol products using manganese complexes in combination with H_2O_2. Pivotal to our findings is the use of sterically encumbered tetradentate aminopyridine ligands in combination with a halogenated carboxylic acid additive and a fluorinated alcohol solvent. We have shown that complexes with bulky ligands perform better in arene oxidations by

preventing coordination of the phenolate products to the manganese center. Remarkably, the use of bulky manganese complexes favors aromatic oxidation over (benzylic) aliphatic C–H bond oxidation, whereas electron-rich manganese complexes selectively oxidize the weaker benzylic C–H bonds, demonstrating a dependency of the chemoselectivity on the catalyst. A synthetically relevant property of the current Mn system is that oxidation of a broad range of aromatic substrates can be accomplished. Notable is the oxidation of monoalkylbenzenes using **Mn(^{tips}bpmcn)** as the catalyst, which to our knowledge provide the highest phenol product yields reported to date for homogeneous catalysts. The overall product profiles of this system, in combination with a negligible KIE effect and the effectiveness of using ^{t}BuOOH as oxidant, overall point towards a metal-based mechanism with no significantly involvement of oxygen-centered radicals. Besides, the observation of a NIH shift indicates that aromatic oxidation with the current system is likely to occur via an arene epoxidation pathway.

Future efforts will be focused on the understanding of the factors that govern product selectivity, as well as of possible catalyst deactivation pathways that lead to the still moderate product yields observed in this study. Additional investigations of the current catalytic system will also focus on a further insight in the overall modest mass balances obtained. Overall, our current findings represent a next step in the design of molecular catalysts for the selective oxidation of aromatic substrates, and provide a stepping stone for the further development of selective oxidation catalysts based on manganese.

Experimental Section

General Procedure for Catalytic Hydroxylation Reaction

A 3 mL or 20 mL vial was charged with: substrate (1 equiv.) and the indicated loading of catalyst and corresponding solvent (0.5 mL or 2 mL). The carboxylic acid was added with indicated loading. The vial was cooled on an ice bath or acetonitrile/dry ice bath, depending on the desired temperature, with stirring. Subsequently, a solution of H_2O_2 in the corresponding solvent (indicated loading, diluted from a 35% H_2O_2 aqueous solution) was delivered by syringe pump over 30 min. After the oxidant addition, the resulting mixture was brought to room temperature, and at this point, a 0.8 M biphenyl solution in CH_3CN (0.5 equiv.) was added as internal standard. The solution was filtered through a Celite©, silica and alumina plug, which was subsequently rinsed with 2×1 mL EtOAc. Then the sample was submitted to GC analysis to determine the mass balance, the conversion, and relative ratio of products by comparison with authentic samples. Yields for ethyl-*p*-benzoquinone, propyl-*p*-benzoquinone and isopropyl-*p*-benzoquinone

were calculated with the response factor of methyl-*p*-benzoquinone.

Detailed experimental procedures and characterization data for all new compounds are described in the supporting information.

CCDC-1994176 contains the supplementary crystallographic data for *(S,S)*-Mn(^{tips}bpbi). These data can be obtained free of charge from The Cambridge Crystallographic Data Centre via www.ccdc.cam.ac.uk/data_request/cif.

Acknowledgements

References

[1] a) M. Costas, K. Chen, L. Que Jr, *Coord. Chem. Rev.* **2000**, *200*, 517–544; b) M. S. Chen, M. C. White, *Science* **2007**, *318*, 783–787; c) W. Nam, *Acc. Chem. Res.* **2007**, *40*, 522–531; d) P. E. Gormisky, M. C. White, *J. Am. Chem. Soc.* **2013**, *135*, 14052–14055; e) R. V. Ottenbacher, E. P. Talsi, K. P. Bryliakov, *ACS Catal.* **2014**, *5*, 39–44; f) D. Shen, C. Miao, S. Wang, C. Xia, W. Sun, *Org. Lett.* **2014**, *16*, 1108–1111; g) W. N. Oloo, L. Que Jr, *Acc. Chem. Res.* **2015**, *48*, 2612–2621; h) G. Olivo, O. Cussó, M. Costas, *Chem. Asian J.* **2016**, *11*, 3148–3158; i) D. Font, M. Canta, M. Milan, O. Cussó, X. Ribas, R. J. M. Klein Gebbink, M. Costas, *Angew. Chem. Int. Ed.* **2016**, *55*, 5776–5779; j) M. Milan, G. Carboni, M. Salamone, M. Costas, M. Bietti, *ACS Catal.* **2017**, *7*, 5903–5911; k) M. Milan, M. Bietti, M. Costas, *ACS Cent. Sci.* **2017**, *3*, 196–204; l) J. Chen, M. Lutz, M. Milan, M. Costas, M. Otte, R. J. M. Klein Gebbink, *Adv. Synth. Catal.* **2017**, *359*, 2590–2595; m) R. V. Ottenbacher, E. P. Talsi, K. P. Bryliakov, *Chem. Rec.* **2018**, *18*, 78–90; n) M. Milan, M. Salamone, M. Costas, M. Bietti, *Acc. Chem. Res.* **2018**, *51*, 1984–1995; o) R. V. Ottenbacher, E. P. Talsi, T. V. Rybalova, K. P. Bryliakov, *ChemCatChem* **2018**, *10*, 5323–5330; p) M. Milan, M. Bietti, M. Costas, *Org. Lett.* **2018**, *20*, 2720–2723; q) B. Qiu, D. Xu, Q. Sun, C. Miao, Y.-M. Lee, X.-X. Li, W. Nam, W. Sun, *ACS Catal.* **2018**, *8*, 2479–2487; r) W. Wang, D. Xu, Q. Sun, W. Sun, *Chem. Asian J.* **2018**, *13*,

2458–2464; s) M. C. White, J. Zhao, *J. Am. Chem. Soc.* **2018**, *140*, 13988–14009; t) B. Qiu, D. Xu, Q. Sun, J. Lin, W. Sun, *Org. Lett.* **2019**, *21*, 618–622; u) J. Zhao, T. Nanjo, E. C. de Lucca Jr, M. C. White, *Nature* **2019**, *11*, 213–221.

[2] a) M. Wu, B. Wang, S. Wang, C. Xia, W. Sun, *Org. Lett.* **2009**, *11*, 3622–3625; b) R. V. Ottenbacher, K. P. Bryliakov, E. P. Talsi, *Adv. Synth. Catal.* **2011**, *353*, 885–889; c) I. Garcia-Bosch, L. Gomez, A. Polo, X. Ribas, M. Costas, *Adv. Synth. Catal.* **2012**, *354*, 65–70; d) O. Cussó, I. Garcia-Bosch, D. Font, X. Ribas, J. Lloret-Fillol, M. Costas, *Org. Lett.* **2013**, *15*, 6158–6161; e) O. Cussó, I. Garcia-Bosch, X. Ribas, J. Lloret-Fillol, M. Costas, *J. Am. Chem. Soc.* **2013**, *135*, 14871–14878; f) R. V. Ottenbacher, D. G. Samsonenko, E. P. Talsi, K. P. Bryliakov, *ACS Catal.* **2014**, *4*, 1599–1606; g) O. Cussó, X. Ribas, M. Costas, *Chem. Commun.* **2015**, *51*, 14285–14298; h) O. Cussó, M. Cianfanelli, X. Ribas, R. J. M. Klein Gebbink, M. Costas, *J. Am. Chem. Soc.* **2016**, *138*, 2732–2738; i) D. Shen, B. Qiu, D. Xu, C. Miao, C. Xia, W. Sun, *Org. Lett.* **2016**, *18*, 372–375; j) J. Du, C. Miao, C. Xia, Y.-M. Lee, W. Nam, W. Sun, *ACS Catal.* **2018**, *8*, 4528–4538; k) C. Clarasó, L. Vicens, A. Polo, M. Costas, *Org. Lett.* **2019**, *21*, 2430–2435; l) M. Mitra, O. Cussó, S. S. Bhat, M. Sun, M. Cianfanelli, M. Costas, E. Nordlander, *Dalton Trans.* **2019**, *48*, 6123–6131; m) M. Borrell, M. Costas, *J. Am. Chem. Soc.* **2017**, *139*, 12821–12829; n) L. Vicens, G. Olivo, M. Costas, *ACS Catal.* **2020**, *10*, 8611–8631.

[3] a) N. Y. Oh, M. S. Seo, M. H. Lim, M. B. Consugar, M. J. Park, J.-U. Rohde, J. Han, K. M. Kim, J. Kim, L. Que Jr, *Chem. Commun.* **2005**, 5644–5646; b) S. Taktak, M. Flook, B. M. Foxman, L. Que Jr, E. V. Rybak-Akimova, *Chem. Commun.* **2005**, 5301–5303; c) A. Thibon, J.-F. Bartoli, R. Guillot, J. Sainton, M. Martinho, D. Mansuy, F. Banse, *J. Mol. Catal. Chem.* **2008**, *287*, 115–120; d) O. V. Makhlynets, E. V. Rybak-Akimova, *Chem. Eur. J.* **2010**, *16*, 13995–14006; e) A. Raba, M. Cokoja, W. A. Herrmann, F. E. Kühn, *Chem. Commun.* **2014**, *50*, 11454–11457; f) A. Kejriwal, P. Bandyopadhyay, A. N. Biswas, *Dalton Trans.* **2015**, *44*, 17261–17267; g) G. Capocasa, G. Olivo, A. Barbieri, O. Lanzalunga, S. Di Stefano, *Catal. Sci. Technol.* **2017**, *7*, 5677–5686; h) A. C. Lindhorst, J. Schütz, T. Netscher, W. Bonrath, F. E. Kühn, *Catal. Sci. Technol.* **2017**, *7*, 1902–1911; i) O. Y. Lyakin, A. M. Zima, N. V. Tkachenko, K. P. Bryliakov, E. P. Talsi, *ACS Catal.* **2018**, *8*, 5255–5260; j) N. V. Tkachenko, R. V. Ottenbacher, O. Y. Lyakin, A. M. Zima, D. G. Samsonenko, E. P. Talsi, K. P. Bryliakov, *ChemCatChem* **2018**, *10*, 4052–4057; k) N. V. Tkachenko, O. Y. Lyakin, A. M. Zima, E. P. Talsi, K. P. Bryliakov, *J. Organomet. Chem.* **2018**, *871*, 130–134; l) S. Kal, A. Draksharapu, L. Que Jr, *J. Am. Chem. Soc.* **2018**, *140*, 5798–5804; m) S. Kal, L. Que Jr, *Angew. Chem. Int. Ed.* **2019**, *58*, 8484–8488; n) S. Xu, A. Draksharapu, W. Rasheed, L. Que Jr, *J. Am. Chem. Soc.* **2019**, *141*, 16093–16107; o) A. M. Zima, O. Y. Lyakin, D. P. Lubov, K. P. Bryliakov, E. P. Talsi, *J. Mol. Catal.*

2020, *483*, 110708; p) X. Wu, M. S. Seo, K. M. Davis, Y.-M. Lee, J. Chen, K.-B. Cho, Y. N. Pushkar, W. Nam, *J. Am. Chem. Soc.* **2011**, *133*, 20088–20091; q) Y. Aratani, Y. Yamada, S. Fukuzumi, *Chem. Commun.* **2015**, *51*, 4662–4665; r) R. V. Ottenbacher, E. P. Talsi, K. P. Bryliakov, *Appl. Organomet. Chem.* **2020**, e5900; s) S. Fukuzumi, K. Ohkubo, *Asian J. Org. Chem.* **2015**, *4*, 836–845.

[4] a) Y. Morimoto, S. Bunno, N. Fujieda, H. Sugimoto, S. Itoh, *J. Am. Chem. Soc.* **2015**, *137*, 5867–5870; b) T. Tsuji, A. A. Zaoputra, Y. Hitomi, K. Mieda, T. Ogura, Y. Shiota, K. Yoshizawa, H. Sato, M. Kodera, *Angew. Chem. Int. Ed.* **2017**, *129*, 7887–7890; c) L. Vilella, A. Conde, D. Balcells, M. M. Díaz-Requejo, A. Lledós, P. J. Pérez, *Chem. Sci.* **2017**, *8*, 8373–8383; d) H. K. Kwong, P. K. Lo, S. M. Yiu, H. Hirao, K. C. Lau, T. C. Lau, *Angew. Chem. Int. Ed.* **2017**, *56*, 12260–12263; e) S. Muthuramalingam, K. Anandababu, M. Velusamy, R. Mayilmurugan, *Catal. Sci. Technol.* **2019**, *9*, 5991–6001; f) S. Muthuramalingam, K. Anandababu, M. Velusamy, R. Mayilmurugan, *Inorg. Chem.* **2020**, *59*, 5918–5928; g) K. Anandababu, S. Muthuramalingam, M. Velusamy, R. Mayilmurugan, *Catal. Sci. Technol.* **2020**, *10*, 2540–2548.

[5] E. Masferrer-Rius, R. M. Hopman, J. van der Kleij, M. Lutz, R. J. M. Klein Gebbink, *Chimia* **2020**, *74*, 489–494.

[6] B. Ticconi, A. Colcerasa, S. Di Stefano, O. Lanzalunga, A. Lapi, M. Mazzonna, G. Olivo, *RSC Adv.* **2018**, *8*, 19144–19151.

[7] a) V. Dantignana, M. Milan, O. Cussó, A. Company, M. Bietti, M. Costas, *ACS Cent. Sci.* **2017**, *3*, 1350–1358; b) R. V. Ottenbacher, D. G. Samsonenko, E. P. Talsi, K. P. Bryliakov, *Org. Lett.* **2012**, *14*, 4310–4313; c) E. P. Talsi, D. G. Samsonenko, R. V. Ottenbacher, K. P. Bryliakov, *ChemCatChem* **2017**, *9*, 4580–4586; d) R. K. Chambers, J. Zhao, C. P. Delaney, M. C. White, *Adv. Synth. Catal.* **2020**, *362*, 417–423.

[8] a) B. P. Roberts, *Chem. Soc. Rev.* **1999**, *28*, 25–35; b) D. Wang, W. G. Shuler, C. J. Pierce, M. K. Hilinski, *Org. Lett.* **2016**, *18*, 3826–3829; c) E. Gaster, S. Kozuch, D. Pappo, *Angew. Chem. Int. Ed.* **2017**, *56*, 5912–5915; d) A. M. Adams, J. Du Bois, *Chem. Sci.* **2014**, *5*, 656–659; e) M. Borrell, S. Gil-Caballero, M. Bietti, M. Costas, *ACS Catal.* **2020**, *10*, 4702–4709; f) R. V. Ottenbacher, E. P. Talsi, K. P. Bryliakov, *J. Catal.* **2020**, *390*, 170–177.

[9] a) Examples of manganese-phenolate complexes: A. Neves, S. M. Erthal, I. Vencato, A. S. Ceccato, Y. P. Mascarenhas, O. R. Nascimento, M. Horner, A. A. Batista, *Inorg. Chem.* **1992**, *31*, 4749–4755; b) S. Wada, M. Mikuriya, *Bull. Chem. Soc. Jpn.* **2008**, *81*, 348–357; c) D. Mandal, P. B. Chatterjee, S. Bhattacharya, K.-Y. Choi, R. Clérac, M. Chaudhury, *Inorg. Chem.* **2009**, *48*, 1826–1835; d) M. Sankaralingam, M. Palaniandavar, *Dalton Trans.* **2014**, *43*, 538–550; e) M. Mikuriya, S. Kurahashi, S. Tomohara, Y. Koyama, D. Yoshioka, R. Mitsuhashi, H. Sakiyama, *Magnetochemistry* **2019**, *5*, 8.

[10] a) E. P. Talsi, K. P. Bryliakov, *Coord. Chem. Rev.* **2012**, *256*, 1418–1434; b) K. P. Bryliakov, E. P. Talsi, *Coord. Chem. Rev.* **2014**, *276*, 73–96; c) O. Y. Lyakin, R. V. Ottenbacher, K. P. Bryliakov, E. P. Talsi, *ACS Catal.* **2012**, *2*, 1196–1202; d) R. V. Ottenbacher, E. P. Talsi, K. P. Bryliakov, *ACS Catal.* **2015**, *5*, 39–44.

[11] a) A. D. Ryabov, I. K. Sakodinskaya, A. K. Yatsimirsky, *J. Chem. Soc. Dalton Trans.* **1985**, 2629–2638; b) M. Lafrance, S. I. Gorelsky, K. Fagnou, *J. Am. Chem. Soc.* **2007**, *129*, 14570–14571; c) A. Maleckis, J. W. Kampf, M. S. Sanford, *J. Am. Chem. Soc.* **2013**, *135*, 6618–6625.

[12] J. W. de Boer, J. Brinksma, W. R. Browne, A. Meetsma, P. L. Alsters, R. Hage, B. L. Feringa, *J. Am. Chem. Soc.* **2005**, *127*, 7990–7991.

[13] pK_a values were taken from: W. M. Haynes, *Handbook of Chemistry and Physics*, 91st ed., CRC Press (Taylor and Francis Group), Boca Raton, FL.

[14] a) D. I. Metelitsa, *Russ. Chem. Rev.* **1971**, *40*, 563; b) C. Walling, R. A. Johnson, *J. Am. Chem. Soc.* **1975**, *97*, 363–367; c) A. Kunai, S. Hata, S. Ito, K. Sasaki, *J. Am. Chem. Soc.* **1986**, *108*, 6012–6016; d) T. Kurata, Y. Watanabe, M. Katoh, Y. Sawaki, *J. Am. Chem. Soc.* **1988**, *110*, 7472–7478.

[15] G. Olivo, O. Lanzalunga, S. Di Stefano, *Adv. Synth. Catal.* **2016**, *358*, 843–863.

[16] a) R. Mas-Ballesté, L. Que, *J. Am. Chem. Soc.* **2007**, *129*, 15964–15972; b) R. V. Ottenbacher, E. P. Talsi, K. P. Bryliakov, *Molecules* **2016**, *21*, 1454.

[17] H. Marusawa, K. Ichikawa, N. Narita, H. Murakami, K. Ito, T. Tezuka, *Bioorg. Med. Chem.* **2002**, *10*, 2283–2290.

[18] a) P. A. MacFaul, K. Ingold, D. Wayner, L. Que, *J. Am. Chem. Soc.* **1997**, *119*, 10594–10598; b) K. U. Ingold, P. A. MacFaul, *Biomimetic oxidations catalyzed by transition metal complexes*, B. Meunier, Ed.; Imperial College Press: London, **2000**; p 45.

[19] R. Hiatt, J. Clipsham, T. Visser, *Can. J. Chem.* **1964**, *42*, 2754–2757.

[20] S. Ito, A. Mitarai, K. Hikino, M. Hirama, K. Sasaki, *J. Org. Chem.* **1992**, *57*, 6937–6941.

[21] R. Augusti, A. O. Dias, L. L. Rocha, R. M. Lago, *J. Phys. Chem. A* **1998**, *102*, 10723–10727.

[22] Z. Siddiqi, W. C. Wertjes, D. Sarlah, *J. Am. Chem. Soc.* **2020**, *142*, 10125–10131.

[23] N. Isaacs, *Pysical Organic Chemistry*, 2nd ed., Longman Scientific, **1995**.

[24] a) P. R. Ortiz de Montellano, *Cytochrome P450: Structure, Mechanism, and Biochemistry 2nd ed.*, ed. (Ed.: P. R. Ortiz de Montellano), Plenum Press, New York, **1995**, pp. 245–303; b) B. Meunier, S. P. De Visser, S. Shaik, *Chem. Rev.* **2004**, *104*, 3947–3980; c) K. R. Korzekwa, D. C. Swinney, W. F. Trager, *Biochemistry* **1989**, *28*, 9019–9027; d) S. P. de Visser, S. Shaik, *J. Am. Chem. Soc.* **2003**, *125*, 7413–7424; e) E. V. Kudrik, A. B. Sorokin, *Chem. Eur. J.* **2008**, *14*, 7123–7126.

[25] K. Feng, R. E. Quevedo, J. T. Kohrt, M. S. Oderinde, U. Reilly, M. C. White, *Nature* **2020**, *580*, 621–627.